Journal of Sound and Vibration (1999) **224**(5), 917–935
Article No. jsvi.1999.2223, available online at http://www.idealibrary.com on IDEAL®

FINITE-ELEMENT ANALYSIS OF THE FLUTTERING PANELS EXCITED BY EXTERNAL FORCES

G. SURACE

Politecnico di Torino, Corso Duca degli Abruzzi 24, 10129 *Torino, Italy*

AND

R. UDRESCU

COMOTI–National Institute for R&D of Turbomachinery, Bd.Iuliu Maniu 220, 76194 *Bucharest, Romania*

(*Received* 15 *December* 1998, *and in final form* 1 *March* 1999)

In this article the classical analysis of the static pressure effect on fluttering panels is extended to cases of pulse and step excitations. A high order finite-element methodology is applied within the non-linear elastic, linear aerodynamic theories and a dynamic analysis is performed on a reference structural model (simply supported isotropic square panel). The results which substantiate this study show that during applied excitation the pattern of the motion is changed into damped or limit-cycle oscillations having non-zero mean value. There are also conditions that could increase limit-cycle flutter amplitudes during excitation and these cases need careful investigations for a reliable structural design.

1. INTRODUCTION

Dynamics and stability of aircraft structures regularly involve non-linear phenomena which can be investigated only through advanced methods of large deflections theory. It is already known that if a panel substructure exposed to aerodynamic forces is also subjected to thermal stresses (due to kinetic heating of the supersonic flow), the non-linear aerothermoelastic behaviour becomes complex even for a relatively simple case [1] (see Figure 1 for a one-dimensional non-linear structural panel model). In the absence of fluid flow, but at sufficiently large compressive load, the plate will buckle into a statically deformed shape whilst, in contrast, for no compressive load, but with a fluid flow of sufficiently large velocity, the plate will flutter with a periodic motion. With both compressive load and fluid flow, chaotic motion may take place.

The general configuration (Figure 2) involves a rectangular panel substructure with fixed edges (clamped or simply supported, with completely immovable in-plane displacements at the edges: $u(0, y) = u(a, y) = v(x, 0) = v(x, b) = 0$), having

0022-460X/99/300917 + 19 $30.00/0

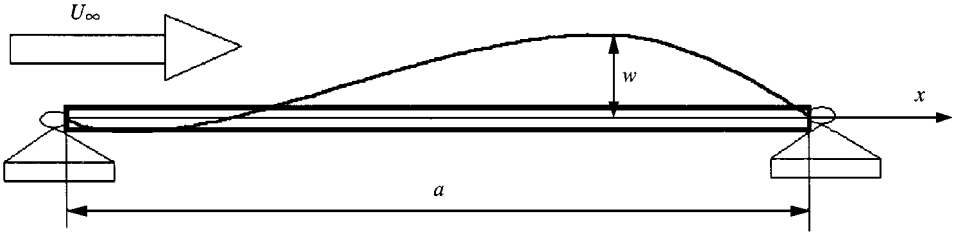

Figure 1. Beam-model for panel flutter.

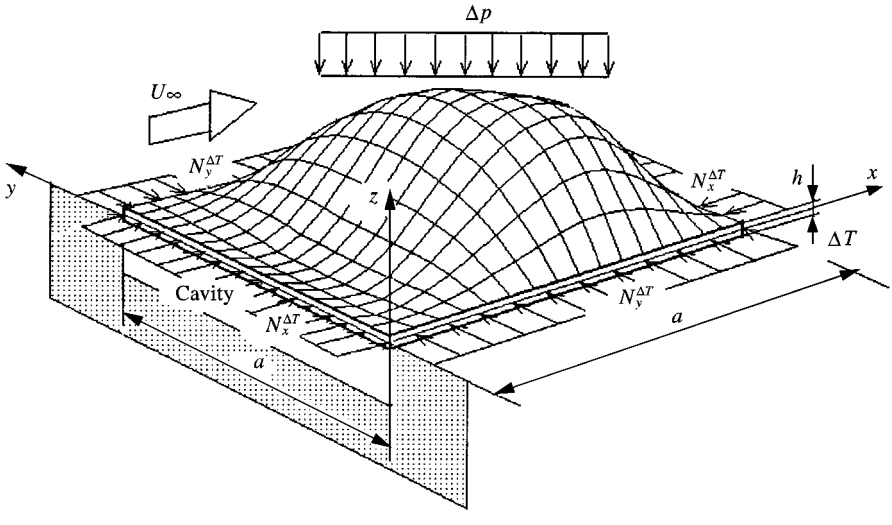

Figure 2. General model for non-linear panel flutter.

the external surface exposed to supersonic flow and the other side facing a cavity. Usually the deflection is the order of plate thickness, but in Figures 1 and 2 it is shown at a greatly exaggerated scale for clarity. The non-linear structural effect, resulting from the in-plane stretching stresses induced by the large amplitudes of the out-of-plane motion, governs the aeroelastic behaviour. Since the tension increases at increasing deflections and remains positive for any sign of the amplitude, a limited aeroelastic response arises at supercritical dynamic pressures. A linear analysis of this case could offer incomplete or erroneous information: critical dynamic pressure, frequency of vibration, and mode shape at the instability can be determined, but usually this yields no direct information about panel deflection and stresses.

The phenomenon has received growing interest due to the development of aircraft and missiles which operate at supersonic speeds. The earliest reported failures that can be attributed to panel flutter were those of the German V-2 rockets during the World War II [2]. Even recently cracks were found in about half of the laminated composite skin of the F-117A stealth fighter [3].

A systematic analysis of the phenomenon began during the 1960s. At that time, the solutions of the non-linear isotropic panel flutter were found usually through

the use of Galerkin's method in the spatial domain and subsequently by numerical integration. Dowell's study [4] provides an overview of this classical method. The next step in the methodological approach was the application of the finite-element method (FEM), firstly to the study of the linear problem [5] and then the extension to the non-linear oscillations of two-dimensional isotropic panels [6, 7] and three-dimensional isotropic plates [8, 9]. Houbolt [10] was the first author who took into account the thermal buckling effect due to the temperature difference between panel and its supports. Usually a constant temperature distribution was considered, but later, in addition to the flutter of 2D- and 3D-isotropic plates, Xue and Mei [11] also considered the effects of arbitrary temperatures.

Recently, a number of studies focused on the non-linear flutter of composite panels (e.g. references [12, 13]). Also, an important research in the field of control and suppression of the non-linear panel flutter is beginning to be developed. Successful application of piezoelectric actuation in this area has already been reported by Mei et al. [14–16].

Until now, no significant work has dealt with the effect of the external forces on the panel flutter behaviour. By considering constant static pressure differential over the simple model from Figure 1, Dowell [1] concluded that there arises a stiffening effect of the plate so that the flutter is completely suppressed. This paper extends the analysis to more complex loads in the form of pulse and step excitation. The pulse pressure could characterize the external loading during launching the missiles originally attached under the wing (Figure 3). The most exposed area is adjacent to the afflux during launch, but the phenomenon can also cause structural damage during the acceleration of the missile. For any weapon it is necessary to know the blast pressure characteristic in order to certify the reliability of the exposed local structure. Experimental validation involves ground tests in which the structure is subjected to pulse forces using mechanical exciters. That is why a more realistic analysis, which includes both aerothermoelastic conditions and external excitation, needs to be addressed. This study investigates the dynamic behaviour which might have implications for the stability and reliability of the structural system.

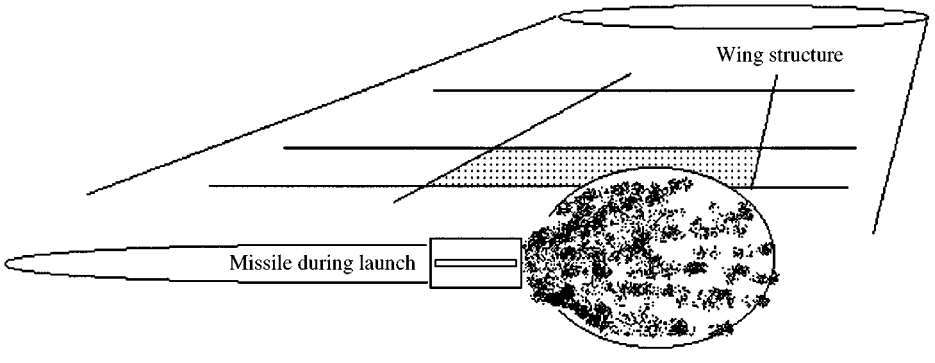

Figure 3. Skew of the local substructure subjected to external out-of-plane pressures.

2. GOVERNING EQUATIONS

An exhaustive formulation of the analytical model within the non-linear elastic and aerodynamic theories can be found in Dowell's monograph [17]. The following considerations show the main steps in modelling the aerothermoelastic problem and its formulation within the finite-element method (FEM).

It is known that the stresses arising in an isotropic Hookean plate (having bending rigidity D, Young's modulus E, Poisson's coefficient v and coefficient of thermal expansion α) subjected to uniform temperature difference ΔT can be written as the sum of the tension created by the stretching of the plate due to bending and the thermal applied in-plane load:

$$\sigma_{xx} = \frac{E}{(1-v^2)}\left[\varepsilon_{xx} + v\varepsilon_{yy}\right] - \frac{E}{(1-v)}\alpha\Delta T,$$

$$\sigma_{yy} = \frac{E}{(1-v^2)}\left[\varepsilon_{yy} + v\varepsilon_{xx}\right] - \frac{E}{(1-v)}\alpha\Delta T,$$

$$\sigma_{xy} = \frac{E}{2(1+v)}\varepsilon_{xy}. \tag{1}$$

The von Karman non-linear strain–displacement relations for a general plate element undergoing both extension and bending at any point z is a sum of membrane and change of curvature strain components:

$$\varepsilon_{xx} = \frac{\partial u}{\partial x} + \frac{1}{2}\left(\frac{\partial w}{\partial x}\right)^2 - z\frac{\partial^2 w}{\partial x^2} = \varepsilon_{xx0} - z\frac{\partial^2 w}{\partial x^2},$$

$$\varepsilon_{yy} = \frac{\partial v}{\partial y} + \frac{1}{2}\left(\frac{\partial w}{\partial y}\right)^2 - z\frac{\partial^2 w}{\partial y^2} = \varepsilon_{yy0} - z\frac{\partial^2 w}{\partial y^2},$$

$$\varepsilon_{xy} = \frac{\partial v}{\partial x} + \frac{\partial u}{\partial y} + \frac{\partial w}{\partial x}\frac{\partial w}{\partial y} - 2z\frac{\partial^2 w}{\partial x \partial y} = \varepsilon_{xy0} - 2z\frac{\partial^2 w}{\partial x \partial y}. \tag{2}$$

Denoting N_x, N_y and N_{xy} the normal and shear tensions, respectively as

$$N_x = \int_{-h/2}^{h/2} \sigma_{xx}\,\mathrm{d}z,$$

$$N_y = \int_{-h/2}^{h/2} \sigma_{yy}\,\mathrm{d}z,$$

$$N_{xy} = \int_{-h/2}^{h/2} \sigma_{xy}\,\mathrm{d}z \tag{3}$$

these can be used in an expression of the strain energy as a sum of stretching and pure bending components:

$$U = \frac{1}{2}\iiint \left[\sigma_{xx}\varepsilon_{xx} + \sigma_{yy}\varepsilon_{yy} + \sigma_{xy}\varepsilon_{xy}\right]\mathrm{d}x\,\mathrm{d}y\,\mathrm{d}z = U_S + U_B. \tag{4}$$

The two terms of the strain energy have been identified as having the following expressions:

$$U_S = \frac{1}{2}\iint [N_x \varepsilon_{xx0} + N_y \varepsilon_{yy0} + N_{xy}\varepsilon_{xy0}]\,\mathrm{d}x\,\mathrm{d}y, \tag{5}$$

$$U_B = \frac{D}{2}\iint \left[\left(\frac{\partial^2 w}{\partial x^2}\right)^2 + \left(\frac{\partial^2 w}{\partial y^2}\right)^2\right]\mathrm{d}x\,\mathrm{d}y + \frac{D}{2}\iint \left[2\nu\frac{\partial^2 w}{\partial x^2}\frac{\partial^2 w}{\partial y^2} + 2(1-\nu)\left(\frac{\partial^2 w}{\partial x\,\partial y}\right)^2\right]\mathrm{d}x\,\mathrm{d}y. \tag{6}$$

The governing equation of the general aeroelastic model is obtained through the application of Hamilton's principle stating an equilibrium between the variation of kinetic energy, strain energy, and the virtual work done by the several aerodynamic pressures:

$$\int (\delta T - \delta U + \delta W)\,\mathrm{d}t = 0. \tag{7}$$

For a rectangular isotropic plate the derivation of equation of equilibrium is detailed by Dowell in reference [17] and may be written in the form

$$D\Delta^2 w - N_x\frac{\partial^2 w}{\partial x^2} - N_y\frac{\partial^2 w}{\partial y^2} + m\frac{\partial^2 w}{\partial t^2} + \Delta p_a = \Delta p_s, \tag{8}$$

where Δp_s and Δp_a are the static and aerodynamic pressures respectively.

The simplest approximation of the aerodynamic forces valid for the domain of hypersonic velocities is sufficient for predicting the aerodynamic terms at high Mach numbers. Moreover, Bailie and McFeely [18] have shown that their results in panel flutter analysis obtained using a full unsteady hypersonic theory agree closely with the results of this approximate theory. The simplified formula of the aerodynamic pressure within the first order "piston theory" [2, 4, 17] obtained supposing the air jet flowing in the x direction has the expression

$$\Delta p_a = \frac{2q_\infty}{M_\infty^2}\left(\frac{\partial w}{\partial x} + \frac{1}{V_\infty}\frac{\partial w}{\partial t}\right), \tag{9}$$

where $q_\infty = \rho_a V_\infty^2/2$ is the dynamic pressure, M_∞ is the Mach number, ρ_α is the air mass density, V_∞ is the free-stream airflow speed and w is the transverse displacement of panel.

The finite-element formulation of the general aerothermoelastic equation can be obtained by using the principle of virtual displacement, stating that if a compatible variation of the displacements $\delta\mathbf{w}$ of a structural finite element with volume loads $\mathbf{p}_v = -m\ddot{\mathbf{w}}$, pressure loads $\mathbf{p}_s$, and inner stresses $\boldsymbol{\sigma}$ takes place, then the inner virtual work must equal the virtual work done by the loads:

$$\int_V \boldsymbol{\sigma}\delta\boldsymbol{\varepsilon}\,\mathrm{d}V = \int_V \mathbf{p}_V^{\mathrm{t}}\delta\mathbf{w}\,\mathrm{d}V + \int_S \mathbf{p}_S^{\mathrm{t}}\delta\mathbf{w}\,\mathrm{d}S \tag{10}$$

By summing up the contributions from all the elements and applying the kinematic boundary conditions, the global system equations of motion for a given rectangular panel can be written in a classical matrix form (see also references [11, 13]) which includes separately the plate and membrane terms (denoted by the subscripts "b" and "m" respectively):

$$\begin{bmatrix} \mathbf{M}^0_{bb} & \mathbf{0} \\ \mathbf{0}^t & \mathbf{M}^0_{mm} \end{bmatrix} \begin{bmatrix} \ddot{\mathbf{W}}^0_b \\ \ddot{\mathbf{W}}^0_m \end{bmatrix} + \sqrt{\frac{\lambda^r \delta}{M_\infty}} \begin{bmatrix} \mathbf{B}^0 & \mathbf{0} \\ \mathbf{0}^t & \mathbf{0} \end{bmatrix} \begin{bmatrix} \dot{\mathbf{W}}^0_b \\ \dot{\mathbf{W}}^0_m \end{bmatrix} + \left(\lambda^r \begin{bmatrix} \mathbf{A}^0 & \mathbf{0} \\ \mathbf{0}^t & \mathbf{0} \end{bmatrix} \right.$$

$$\left. + \begin{bmatrix} \mathbf{K}^0_{bb} + \sigma_x \mathbf{K}^0_g & \mathbf{0} \\ \mathbf{0}^t & \mathbf{K}^0_{mm} \end{bmatrix} + \begin{bmatrix} \mathbf{K}^0_{1bb} & \mathbf{K}^0_{1bm} \\ \mathbf{K}^0_{1mb} & \mathbf{0} \end{bmatrix} + \begin{bmatrix} \mathbf{K}^0_{2bb} & \mathbf{0} \\ \mathbf{0}^t & \mathbf{0} \end{bmatrix} \right) \begin{bmatrix} \mathbf{W}^0_b \\ \mathbf{W}^0_m \end{bmatrix} = \begin{bmatrix} p\mathbf{P}^0_s \\ \mathbf{0} \end{bmatrix}, \quad (11)$$

where $\mathbf{M}$, $\mathbf{B}$, $\mathbf{A}$ and $\mathbf{K}$ are the mass, aerodynamic damping, aerodynamic influence, and linear stiffness matrices, respectively, $\mathbf{K}_g$ is the geometric stiffness due to thermal forces, $\mathbf{K}_1$ and $\mathbf{K}_2$ are the non-linear stiffness matrices that depend linearly and quadratically on the system nodal displacement vector $\mathbf{W}$, respectively, $\mathbf{P}_S$ is the externally applied out-of-plane load vector, assumed as transverse-distributed pressure with non-dimensional amplitude p, defined by Dowell's notation. In equation (11) the non-dimensionality proposed by Dowell [4] (denoted by superscript "o") is obtained by using dimensionless time τ, deflection W, dynamic pressure λ^r, buckling loads σ_x, σ_y and transversal pressure p:

$$\zeta = t\sqrt{\frac{D}{ma^4}}, \qquad W = \frac{w}{h}, \lambda^r = \frac{\rho_\infty U^2_\infty a^3}{M_\infty D}, \qquad \delta = \frac{\rho_\infty a}{m},$$

$$\sigma_x = \frac{N^{\Delta T}_x a^2}{D}, \sigma_y = \frac{N^{\Delta T}_y a^2}{D}, p = \frac{\Delta p_s a^4}{Dh}. \quad (12)$$

This has the advantages of expressing the various results in a compact form and establishes scaling laws to extrapolate results for other physical situations. If the edges are completely restrained against the in-plane motion, the in-plane stress resultants $N^{\Delta T}_x$ and $N^{\Delta T}_y$ are equal and the buckling parameters for a square panel of length a are equal $\sigma_x = \sigma_y$ and are denoted uniquely by σ_x.

The finite-element model proposed by the authors has already been used in performing the classical analysis [19] of the non-linear panel flutter. Mainly, it consists of the Argyris' high order triangular finite element TUBA6 and TRIM6 [20] (fully compatible elements for the out-of-plane w and, respectively, in-plane u, v displacements, respectively, based on the natural geometry concept).

Two nets of identical topology and material properties create the finite-element model. The first is composed of fifth order (six nodes) triangular plate elements. The vector $\mathbf{w}_b$ of 21 nodal degrees of freedom (d.o.f.) of this element consists of displacement w, all first and second derivatives $w_{,x}$, $w_{,y}$, $w_{,xx}$, $w_{,xy}$, $w_{,yy}$ at the vertices (for satisfying the continuity condition in curvature) and the normal derivative $w_{,n}$ at the middle-points of the edges. The plate element has flexural

stiffness and can be loaded by two-dimensional forces (mostly by internal bending and torsional moments and by transverse shears).

The other is composed of a second order triangular membrane elements. The corresponding vector $\mathbf{w}_m$ contains 12 nodal degrees of freedom per element (in-plane displacements u and v at each node). This element has no flexural stiffness and carries loads by axial and central shear forces.

In total there are 33 nodal degrees of freedom per complex plate-membrane element. Detailed presentations of the computational techniques including the matrix formulation of each term of the general equation (11) can be found in reference [21].

3. RESULTS

The numerical study is performed by using an original computational program (written in FORTRAN, with an additional MATHEMATICA module) which has proved its usefulness in solving panel flutter problems of increasing complexity. These included preliminary accuracy tests for the linear elastic, dynamic, and buckling problems of plates under various boundary conditions from which an optimal FE mesh (Figure 4 shows an eight complex plate-membrane triangular elements mesh) resulted with a reduced number of active degrees of freedom of the global displacement vector $\mathbf{W}$: 54 d.o.f.s for a simply supported isotropic square panel.

Also the linear aeroelastic problem (critical dynamic pressure) and the effect of the non-linear elasticity have been investigated with improved acuracy [22]. This

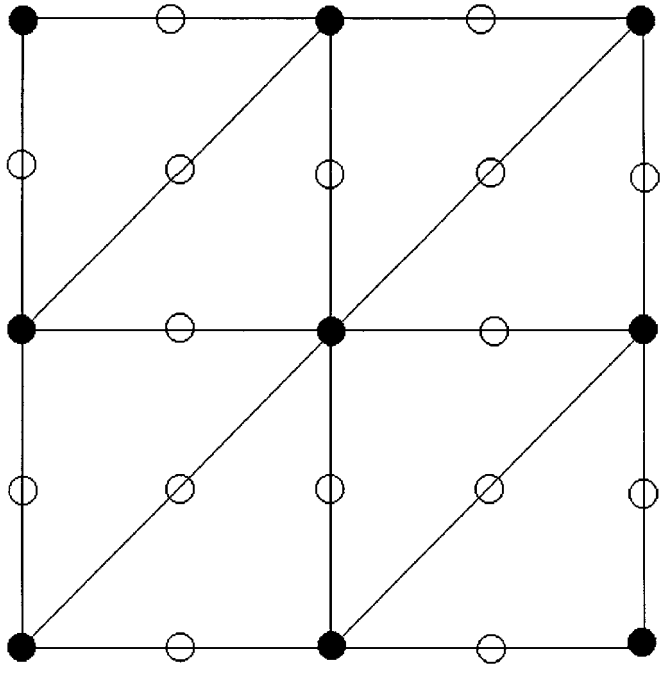

Figure 4. FE mesh. ●—modes with eight d.o.f.s: u, v, w, $w_{,x}$, $w_{,y}$, $w_{,xx}$, $w_{,xy}$, $w_{,yy}$; ○—modes with three d.o.f.s: u, v, w_n

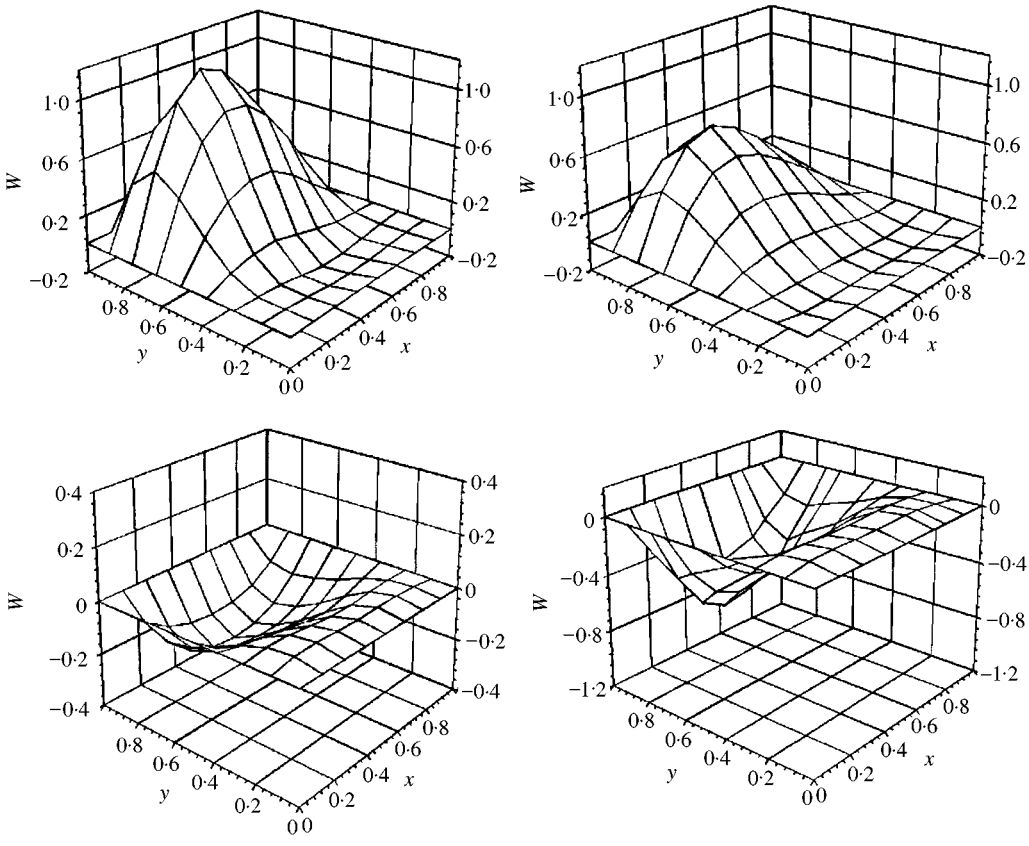

Figure 5. Limit-cycle oscillations of the panel ($\lambda^r = 800$, $\Delta T/\Delta T_{cr} = 0$).

effect involves a limited aeroelastic response limit cycle flutter (Figure 5) arising at supercritical dynamic pressures.

The complete behaviour of the simply supported isotropic square panel under uniform temperature change ΔT (usually in the supercritical buckling domain $\Delta T > \Delta T_{cr}$) arising between panel and its supports at high supersonic flow is represented in the classical map of stability boundaries (Figure 6). This is governed by the non-dimensional parameters of compressive load σ_x and dynamic pressure λ^r. Performing detailed numerical investigation with a fine variation of parameters, as well as integration over an extended time-span, the results confirmed similar maps [4, 11], having four stability regions.

This classical analysis deals with the panel flutter phenomenon describing self-excited oscillations. The new approach now searches for the dynamic behaviour whilst applying external excitation on this model. The investigations are performed on the same structural model by adding external out-of-plane distributed forces in the non-linear aerothermoelastic equation system (11). The models of mono and periodic pulses, and step pressures are taken into account. The non-dimensional damping parameter is set to $\delta/M_\infty = 0{\cdot}01$ and the in-plane inertia term $\mathbf{M}^0_{mm}$ has been neglected. The equation is integrated step-by-step for

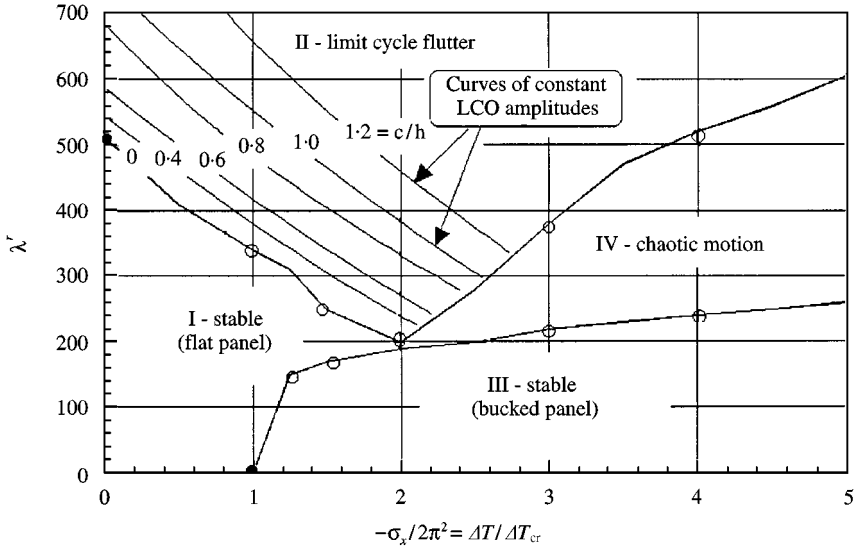

Figure 6. Map of the aerothermoelastic stability boundaries.

certain thermal and dynamic pressure conditions ($\sigma_x/2\pi = -\Delta T/\Delta T_{cr}$ and λ^r, respectively), and external loading. Non-dimensional solutions (dynamic responses at the centre point of the panel, amplitude scaled to panel thickness, dimensionless time and pressure, corresponding to the Dowell's notations) of each stability region are investigated in time domain and significant results are shown together with the excitation (graphic below the dynamic response). Although the mid-point of the plate is not the location of the maximum amplitude which tends to be at the trailing edge (see Figure 5), the pattern of the motion remains the same. The computational program offers capabilities for multiple analyses by combining various parameters ($\sigma_x/2\pi = -\Delta T/\Delta T_{cr}$ and λ^r) with excitations. The following results are obtained by taking into account an example of maximum level of the pressure parameter ($p = 5{\cdot}2$) as representative for all stability areas of a square panel with thickness/length ratio $h/a = 0{\cdot}01$.

The aeroelastic responses due to pulse excitation in limit-cycle oscillations (LCO) domain (2nd region in Figure 6) are presented in Figures 7, and 8 for cases without and with the thermal effect respectively. The pattern of the motions (LCO) remains the same in both cases after the pulse input, but during pulse excitation the behaviours differ; the pulse damps the vibration in the first case (Figure 7) and the oscillation continues in the second case (Figure 8). This observation is valid also in the case of periodic pulses (Figures 9, and 10) at the same flight conditions. In the case of step excitation without thermal effect (Figure 11), the presence of the out-of-plane pressures has a damping effect on the vibrations, determining a static deformed shape of the panel. This stiffening effect, sufficiently so that flutter is completely suppressed, has already been confirmed by Dowell [1] for the one-dimensional structural model. But the presence of the thermal buckling loads emphasises another interesting phenomenon (Figure 12); the flutter behaviour is maintained, and the LCO amplitudes even increase compared with the initial

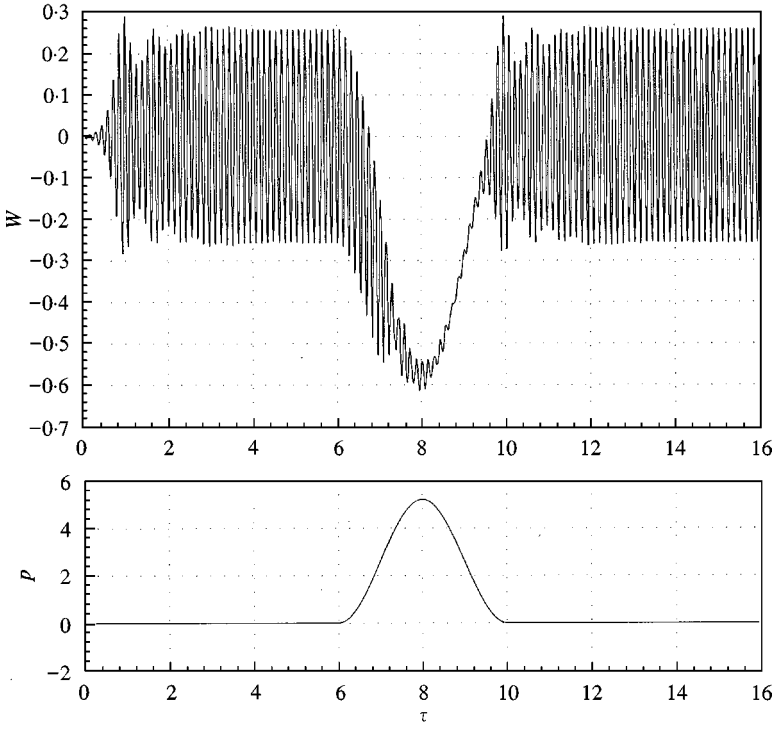

Figure 7. Dynamic behaviour during pulse pressure, LCO-domain ($\Delta T/\Delta T_{cr} = 0$, $\lambda^r = 600$).

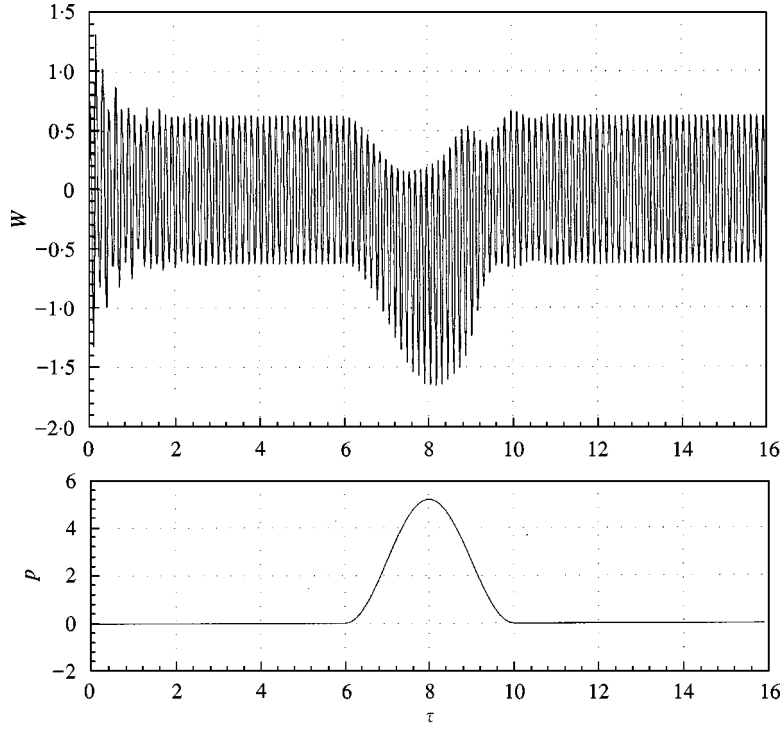

Figure 8. Dynamic behaviour during pulse pressure, LCO-domain ($\Delta T/\Delta T_{cr} = 1$, $\lambda^r = 600$).

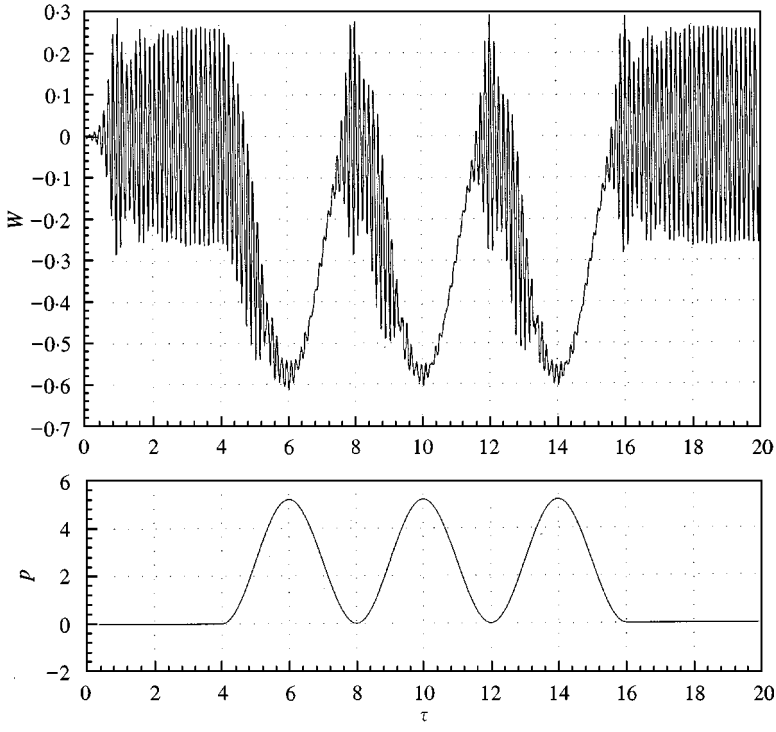

Figure 9. Dynamic behaviour during periodic pulses, LCO-domain ($\Delta T/\Delta T_{cr} = 0$, $\lambda^r = 600$).

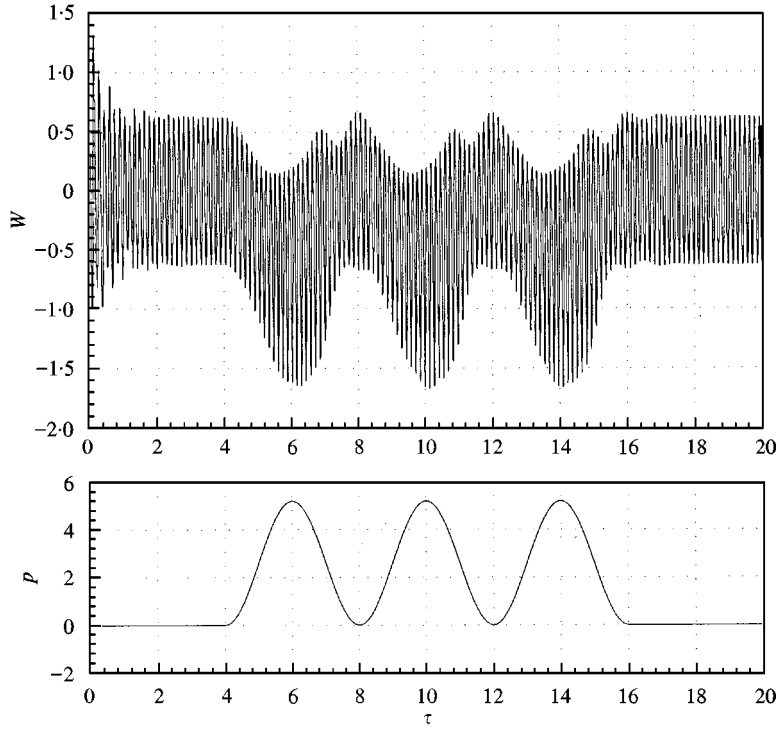

Figure 10. Dynamic behaviour during pulses, LCO-domain ($\Delta T/\Delta T_{cr} = 1$, $\lambda^r = 600$).

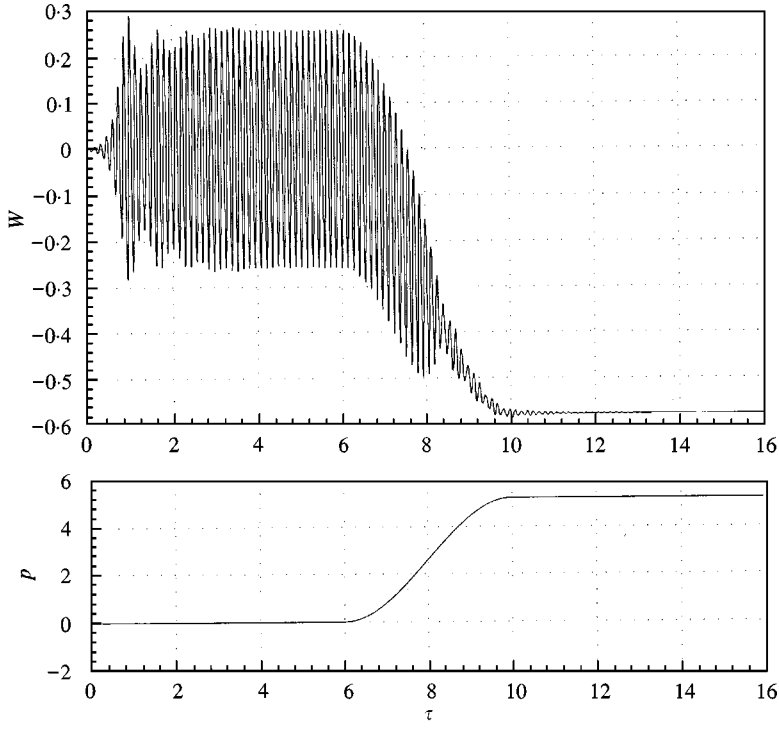

Figure 11. Dynamic behaviour during step pressure, LCO-domain ($\Delta T/\Delta T_{cr} = 0$, $\lambda^r = 600$).

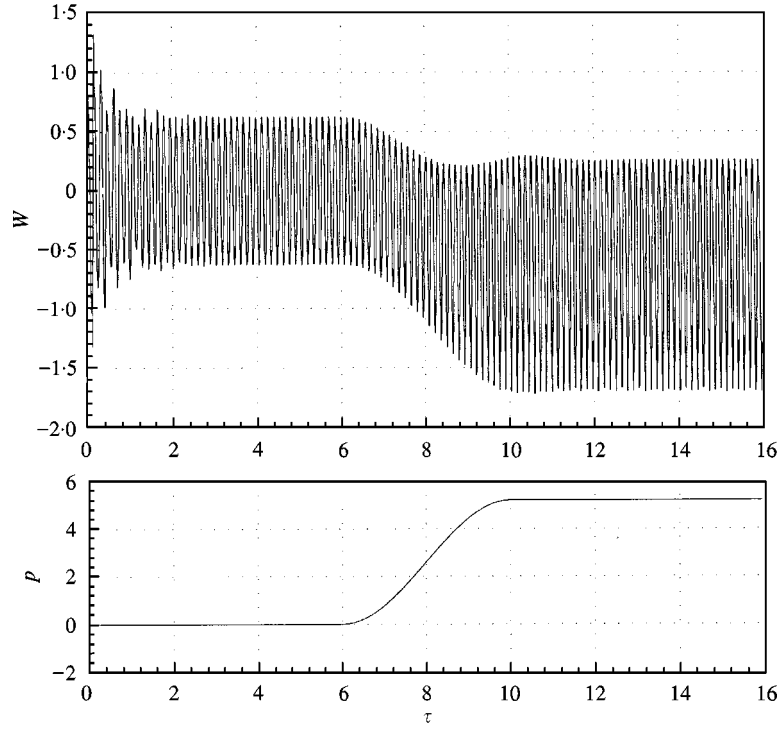

Figure 12. Dynamic behaviour during step pressure, LCO-domain ($\Delta T/\Delta T_{cr} = 1$, $\lambda^r = 600$).

motion. Also the oscillations are shifted during applying out-of-plane loads. These behaviours can be better understood by investigating the corresponding phase plots of the motions under step excitation. Thus, the case of zero-in-plane load is shown in Figure 13 where the ellipse centred about the origin is the trajectory of the initial limit-cycle oscillation. As the pressure is increased, the ellipse decreases in size, moving to the left and finally collapses completely to a point. The inclusion of temperature difference (Figure 14) shows that the initial ellipse centred about the origin (the trajectory of LCO motion before excitation) is increasing in size during excitation, moving to the left and destroying the symmetry until a closed curve is stabilized.

The chaotic domain is investigated in Figures 15–17. The pulse excitation does not change the pattern of the motion (Figure 15), but the step pressures could have an attenuation effect on the oscillations (Figure 16) which are also shifted to a deformed shape of the panel (the mid-position of vibration is not zero). At small dynamic pressures the vibrations become smaller in amplitude (Figure 16) compared to the case of large dynamic pressures (Figure 17). It should be noted that the chaotic motion is sensitive to the initial conditions and small changes of the initial disturbance amplitude determine new patterns of motion. These results give qualitative information about the dynamic behaviour.

The domains of the flat and buckled panel (1st and 3rd, respectively, in Figure 6) also remain stable in the case of pulse excitations (see Figures 18 and 19) because the applied external loads have the effect of a perturbation on a damped system.

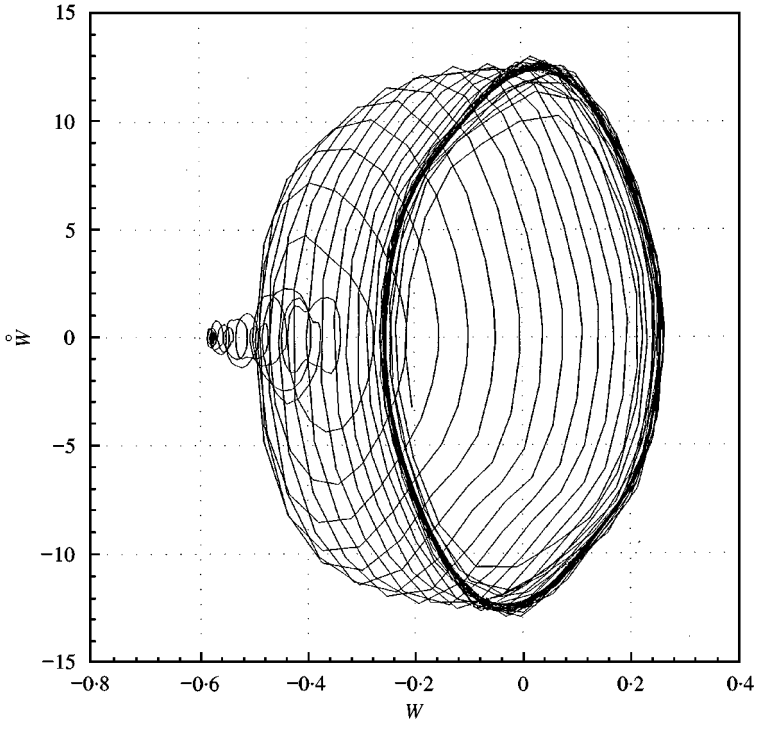

Figure 13. Phase plane plot: effect of step pressure ($\Delta T/\Delta T_{cr} = 0$, $\lambda^r = 600$).

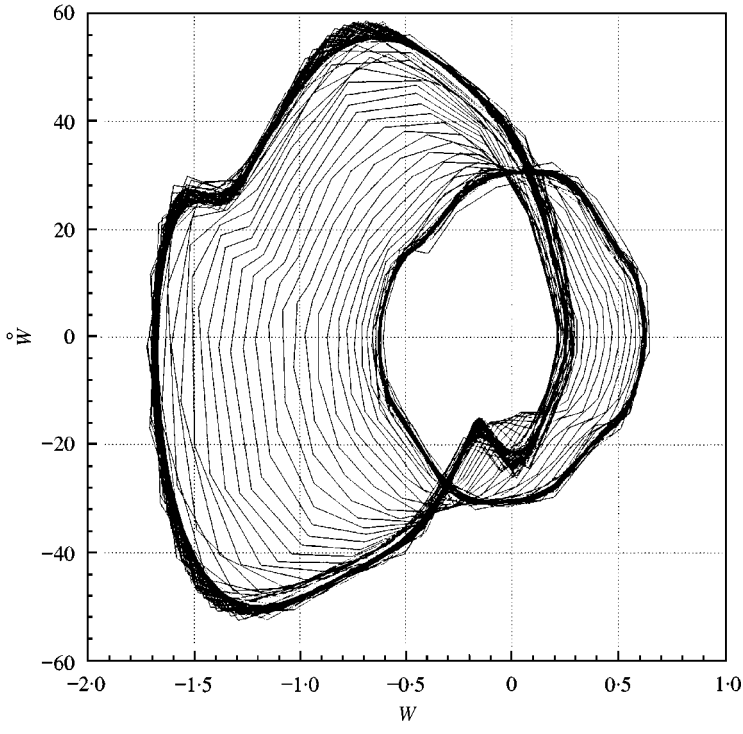

Figure 14. Phase plane plot: effect of step pressure ($\Delta T/\Delta T_{cr} = 1$, $\lambda^r = 600$).

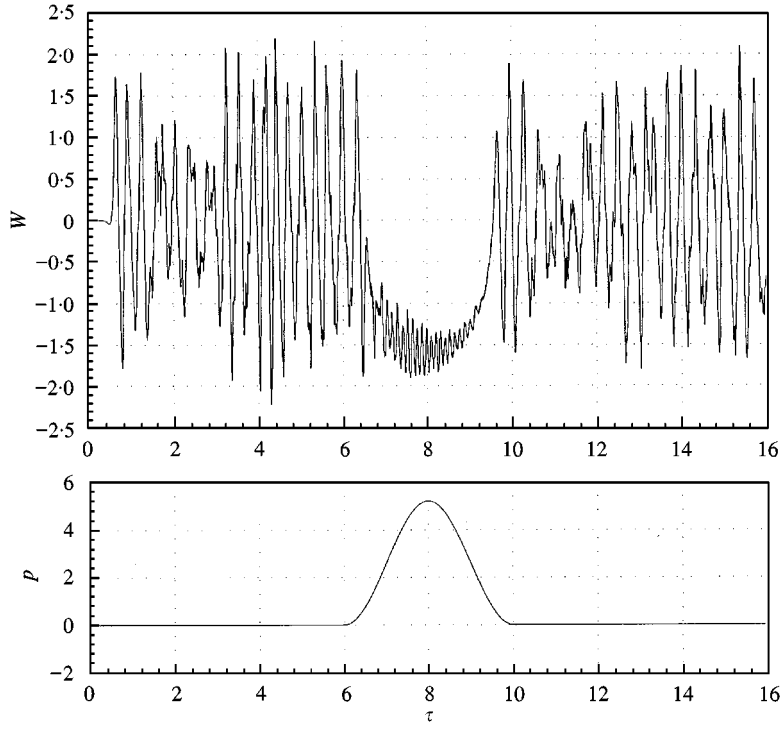

Figure 15. Dynamic behaviour during pulse pressure, chaotic-domain ($\Delta T/\Delta T_{cr} = 3$, $\lambda^r = 300$).

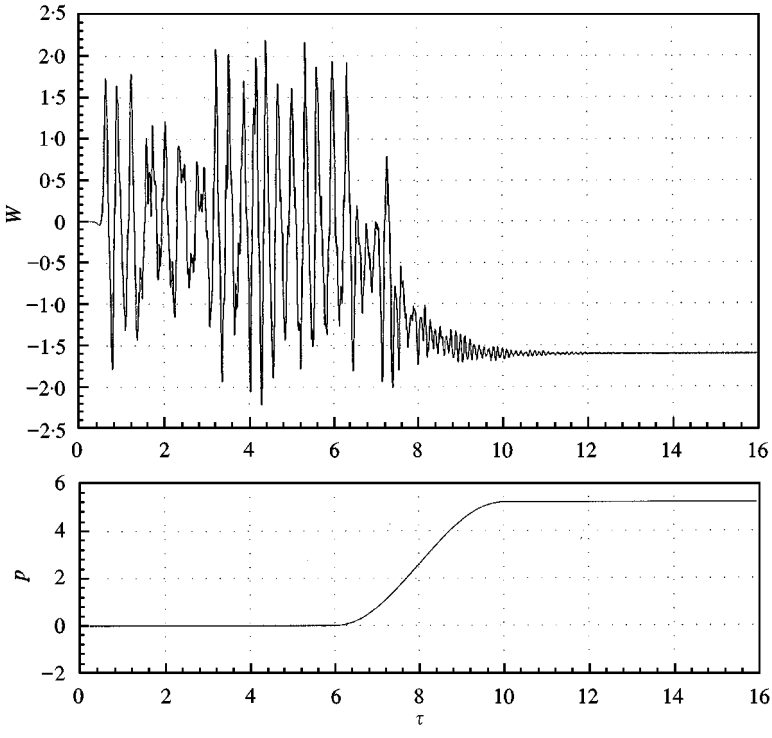

Figure 16. Dynamic behaviour during step pressure, chaotic-domain ($\Delta T/\Delta T_{cr} = 3$, $\lambda^r = 300$).

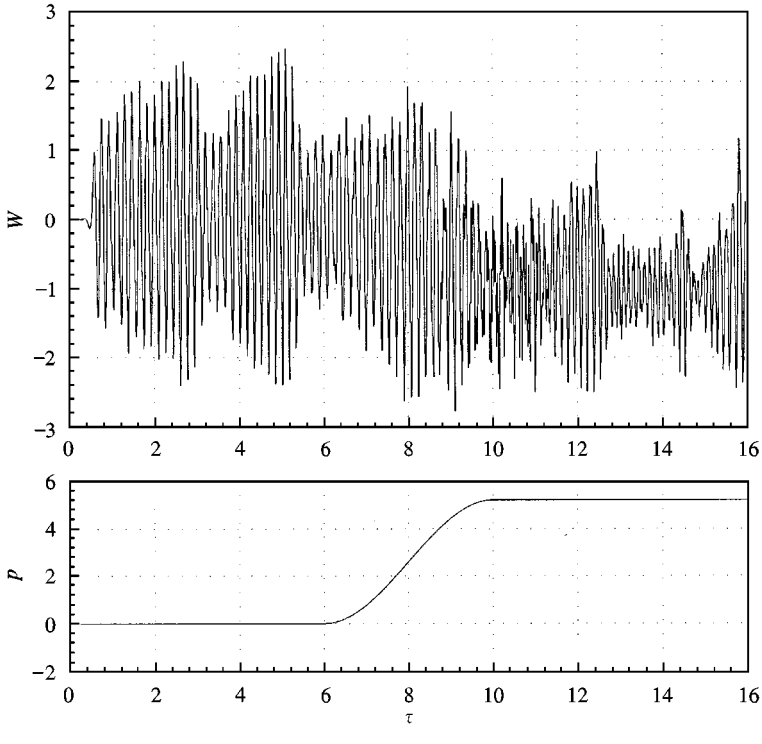

Figure 17. Dynamic behaviour during step pressure, chaotic-domain ($\Delta T/\Delta T_{cr} = 2.5$, $\lambda^r = 500$).

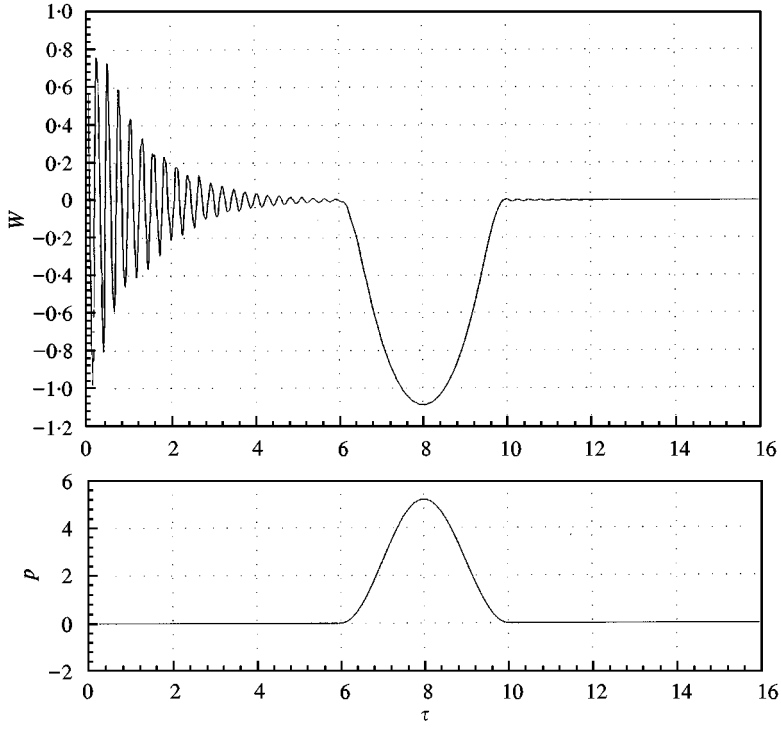

Figure 18. Dynamic behaviour during pulse pressure, stable-flat panel domain ($\Delta T/\Delta T_{cr} = 1$, $\lambda^r = 300$).

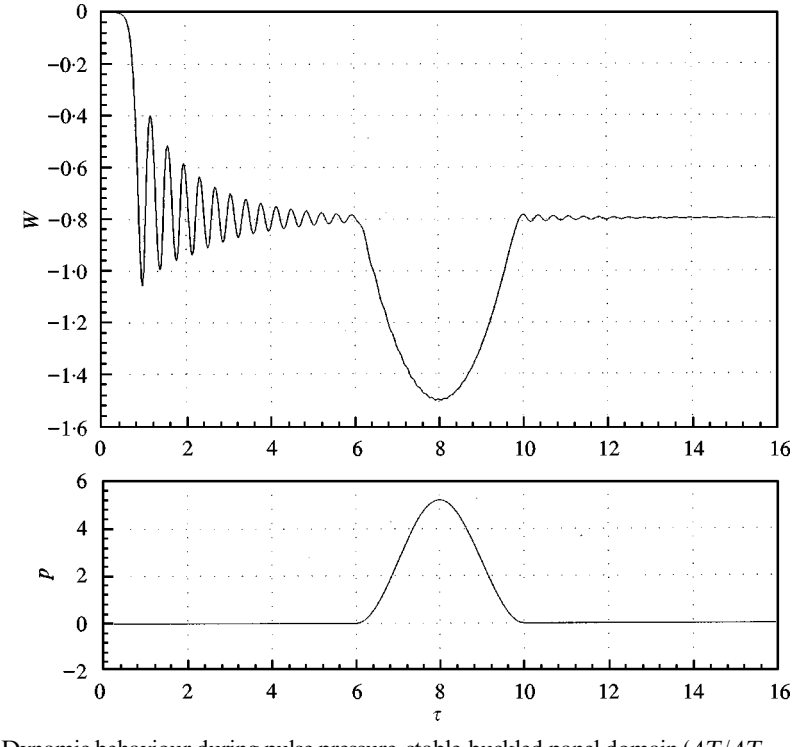

Figure 19. Dynamic behaviour during pulse pressure, stable-buckled panel domain ($\Delta T/\Delta T_{cr} = 2$, $\lambda^r = 150$).

TABLE 1

h/a	Aluminium alloy	Steel
0·004	t (s) $= 0{\cdot}161\tau$ Δp_s (Pa) $= 1{\cdot}724p$	t (s) $= 0{\cdot}159\tau$ Δp_s (Pa) $= 4{\cdot}926p$
0·005	t (s) $= 0{\cdot}129\tau$ Δp_s (Pa) $= 4{\cdot}347p$	t (s) $= 0{\cdot}127\tau$ Δp_s (Pa) $= 12{\cdot}019p$
0·01	t (s) $= 0{\cdot}0645\tau$ Δp_s (Pa) $= 67{\cdot}567p$	t (s) $= 0{\cdot}0637\tau$ Δp_s (Pa) $= 192{\cdot}30p$

The above dimensionless analysis gives information about the qualitative effects of external excitations on the pattern of the motion resulted; oscillations having amplitude scaled to panel thickness, 'frequency" related to non-dimensional time τ, non-dimensional pressure p. In order to have quantitative information it is necessary to perform the dimensional analysis by correlating the dimensionless parameters (time τ and pressure p) with data of panel geometry and material. Thus, the dimensional values of time t (s) and pressure Δp_s (Pa) can be extracted from the Dowell's equations (12):

$$t \text{ (s)} = \frac{a^2}{h}\sqrt{\frac{12(1-\nu^2)\rho}{E}}\,\tau \tag{13}$$

and

$$\Delta p_s \text{ (Pa)} = \frac{E}{12(1-\nu^2)}\left(\frac{h}{a}\right)^4 p \tag{14}$$

respectively.

Two materials, aluminium alloy ($E = 0{\cdot}735 \times 10^{11}$ Pa, $\rho_{\text{Al}} = 2767\ \text{kg/m}^3$) and stainless steel ($E = 2{\cdot}1 \times 10^{11}$ Pa, $\rho_{\text{St}} = 7800\ \text{kg/m}^3$), respectively, are used as examples with three values of thickness ($h/a = 0{\cdot}004$; 0·005; 0·01) of isotropic square panels ($a = 1$ m). Table 1 shows the scale factors for dimensional time and pressure axes.

Examination of these results shows that a relatively small amplitude of external pressure can change the pattern of the motion. Of course, the nearest local substructure exposed to the blast pressure (which is usually significant greater) is strongly stiffened, but the loading effects during ignition, launch and acceleration can influence a wide structural area.

4. CONCLUSIONS

The model of the non-linear panel flutter has been extended to the case of external excitations due to the pulse and step out-of-plane pressures that could appear on local structures during launch of missiles at high speeds. A high order finite-element methodology has been applied within the non-linear elastic, linear

aerodynamic theories and a dynamic analysis has been performed on a reference structural model (simply supported isotropic square panel).

The results which substantiate this study show that in most cases the pattern of the motion is changed during applied excitation into damped or limit-cycle oscillations deflected from its flat state. There are also conditions that could increase limit-cycle flutter amplitudes during excitation and these cases need careful investigation for a reliable structural design of high-speed vehicles.

ACKNOWLEDGMENT

This work has been supported by a grant from the Italian Consiglio Nazionale delle Ricerche, under the NATO Senior Guest Fellowship Programme. The Romanian author wishes to thank the Department of Aeronautical and Space Engineering of the POLITECNICO DI TORINO for the computer facilities and for the help in preparing this manuscript.

REFERENCES

1. E. H. Dowell and M. Ilgamov 1988 *Studies in Nonlinear Aeroelasticity*. Berlin: Springer.
2. R. L. Bisplinghoff and H. Ashley 1962 *Principles of Aeroelasticity*. New York: Wiley.
3. R. Backer 1992 *Plenary Session 8 AIAA Dynamics Specialists Conference*, Dallas. F-117A structures and dynamics design.
4. E. H. Dowell 1970 *AIAA Journal* **8**, 385–399. Panel flutter: a review of the aeroelastic stability of plates and shells.
5. M. D. Olson 1970 *AIAA Journal* **8**, 747–752. Some flutter solutions using finite elements.
6. C. Mei 1977 *AIAA Journal* **15**, 1107–1110. A finite element approach for nonlinear panel flutter.
7. C. E. Gray, C. Mei and C. P. Shore 1991 *AIAA Journal* **29**, 290–298. Finite-element method for large-amplitude two-dimensional panel flutter at hypersonic speeds.
8. C. Mei and H. C. Wang 1982 *Proceedings of the International Conference on Finite Element Method, Shanghai, China, New York: Gordon & Breach*, 944–951. Finite element analysis of large amplitude supersonic flutter of panels.
9. A. D. Han and T. Y. Yang 1983 *AIAA Journal* **21**, 1453–1461. Nonlinear panel flutter using high-order triangular finite elements.
10. J. C. Houbolt 1958 *Ph.D. Thesis Eidenössischen Technichen Hochschule, Swiss Federal Inst. of Technology, Zürich, Switzerland*. A study of several aerothermoelastic problems of aircraft structures in high-speed flight.
11. D. Y. Xue and C. Mei 1993 *AIAA Journal* **31**, 154–162. Finite element nonlinear panel flutter with arbitrary temperatures in supersonic flow.
12. R. I. Dixon and C. Mei 1993 *AIAA Journal* **31**, 701–707. Finite element analysis of large-amplitude panel flutter of thin laminates.
13. R. C. Zhou, Y. Xue and C. Mei 1994 *AIAA Journal* **32**, 2044–2052. Finite element time domain–modal formulation for nonlinear flutter of composite panels.
14. Z. Lai, D. Xue, J-K. Huang and C. Mei 1995 *Journal of Intelligent Material Systems and Structures* **6**, 274–282. Panel flutter limit-cycle suppression with piezoelectric actuation.
15. R. C. Zhou, Z. Lai, D. Xue, J-K. Huang and C. Mei 1995 *AIAA Journal* **33**, 1098–1105. Suppression of nonlinear panel flutter with piezoelectric actuators using finite element method.

16. R. C. Zhou, C. Mei and J-K. Huang 1996 *AIAA Journal* **34**, 347–357. Suppression of nonlinear panel flutter at supersonic speeds and elevated temperatures.
17. E. H. Dowell 1974 *Aeroelasticity of Plates and Shells*. Dordrecht: Kluwer Academic Publishers.
18. J. A. Bailie and J. E. McFeely 1968 *AIAA Journal* **6**, 332–337. Panel flutter in hypersonic flow.
19. R. Udrescu 1998 *A Collection of Technical Papers of the 39th AIAA/ASME/ASCE/AHS/ACS Structures, Structural Dynamics and Materials Conference* **2**, 1252–1262, *AIAA paper* #98–1843. A higher finite element model in nonlinear panel flutter analysis.
20. J. Argyris and H. P. Mlejnek 1986–1988 *Die Metode der Finiten Elementen* (3 vols.). *Braunschweig/Wiesbaden.*
21. J. Argyris and R. Udrescu 1993 *Technical Report, Institute for Computer Applications, University of Stuttgart*. Nonlinear panel flutter on high-order FE model–natural approach.
22. R. Udrescu 1996 *Ph.D. Dissertation, Aerospace Department*, "*Politehnica*" *University of Bucharest*. Contributions to the aeroelasticity of panels modeled by high-order finite elements (in Romanian).